LOW POWER RED LASER IRRADIATION EFFECTS, AS SEEN IN METABOLICALLY INTACT AND IMPAIRED HUMAN BLOOD CELLS

EVA KATONA[*], *GYÖNGYVÉR KATONA*[**], *A. CĂPLĂNUŞI*[**], *I.O. DOAGĂ*[*], *DIANA IONESCU*[*], *R. MATEI*[*], *JUDIT HORVÁTH*[***], *E. TRUȚIA*[**], *E. TANOS*[***], *L. KATONA*[*]

*Department of Biophysics, "Carol Davila" University of Medicine and Pharmaceutics, Bucharest, Romania
** Department of Medical Biochemistry, "Carol Davila" University of Medicine and Pharmaceutics, Bucharest, Romania
***Lasereuropa, OPTIKOP CO., Budapest, POB 405, Hungary

Abstract. The aim of the present work was to contribute to the understanding of the cellular and molecular mechanisms involved in low power long wavelength laser irradiation effects. Investigating the 680 nm laser light influence on the anisotropy of 1,6-diphenyl-1,3,5-hexatriene (DPH) and 1-[(4-trimethyl-amino)phenyl]-6-phenyl-1,3,5-hexatriene (TMA-DPH) fluorescence, we report low power red laser induced changes in the lipid order parameter in various regions of the plasma membrane of human platelets and peripheral blood lymphocytes. Using irradiation doses of therapeutic significance, the dependence of the observed membrane effects on the actual metabolic state of cells is pointed out.

Key words: AlGaInP/GaAs, steady state fluorescence anisotropy, fluorescent lipid probes, plasma membrane fluidity, serum starvation, metabolic impairment, human peripheral lymphocytes, human platelets.

INTRODUCTION

After some 30 years of debate, at present, low power laser therapy (LPLT), also named low level laser therapy (LLLT), became part of physiotherapy in most countries. It is successfully used whenever the goal is promotion of wound healing, reduction of inflammation, and/or pain relief [1, 5, 18, 24, 26–27, 30]. There is no doubt nowadays, that low-intensity monochromatic light from lasers acts directly on the organism at the molecular level [8–14], nonetheless – in spite of the growing number of well designed scientific investigations [2, 12–14, 20–22, 28–29] – the detailed molecular and cellular mechanisms involved remain elusive [13]. There is widely accepted that there exists a universal photobiological mechanism of light action on respiratory chain in both eukaryotic and prokaryotic cells, terminal

Received September, 2004;
in final form December 2004

ROMANIAN J. BIOPHYS., Vol. 13, Nos. 1–4, P. 1–15, BUCHAREST, 2003 ?

enzymes of the respiratory chain being the photoacceptors [8–10, 12–13], and specificity of cellular responses only appearing during secondary reactions [9, 12–14], the cellular membrane being part of the photosignal transduction and amplification chain [13–14]. Irradiation supposedly causes the cellular redox balance to shift toward a more oxidized state (slight oxidative stress), it also optimizes the energy status of a cell [13].

However, there are many still unknown ways how metabolic pathways in a cell are regulated. Therefore, it is not surprising that understanding of light regulation mechanisms of cell metabolism is yet fragmentary [13–14]. Consequently, many short term and long term effects of irradiation should be thoroughly investigated before low power laser therapy will really become a mainstream medical tool.

The aim of the present work was to contribute to the enrichment of the scientific knowledge concerning characteristics and mechanisms involved in soft laser irradiation effects at subcellular level.

Dynamic rearrangement of membrane components at the cell surface and the changes induced in the membrane physico-chemical properties play an essential role in cellular signaling [16, 23]. Multiple cell membrane alterations have been described in humans and animals with various pathologies as well as under the influence of various physico-chemical factors [17, 23]. Using human platelets and peripheral blood lymphocytes, and the lipid probes DPH and TMA-DPH, selected to monitor fluidity/lipid packing density in the core and in the polar headgroup regions of the plasma membrane lipid bilayer respectively, we report steady-state fluorescence anisotropy data revealing membrane effects of the 680 nm laser light. Data analysis is focused on revealing the modulation of the observed lipid order / membrane fluidity changes by the cells actual metabolic state.

MATERIALS AND METHODS

MATERIALS

wrong grammaticaly

The fluorescent lipid probes 1,6-diphenyl-1,3,5-hexatriene (DPH) and 1[4-(trimethylammonium)phenyl]-6-phenyl-1,3,5-hexatriene (TMA-DPH) was from Molecular Probes, Hepes buffer substance from Sigma Chemical Co., while all other chemicals were the best research grade available.

CELLS

Peripheral lymphocytes and platelets were prepared from freshly drawn human blood obtained from healthy volunteers who had not received any medical treatment within two weeks before experiment. The blood was collected in a citrate

buffer (100 mM sodium citrate, 7 mM citric acid, 140 mM glucose, pH 6.5) containing 0.1 mM aspirin. Lymphocytes were separated by Ficoll-Hypaque density gradient centrifugation, washed twice by centrifugation / resuspension / centrifugation at 100g for 5 min, and finally resuspended in Hepes buffer HPMI (buffer no. 1, constituted of 100 mM NaCl, 5.4 mM KCl, 0.4 mM $MgCl_2$, 0.04 $CaCl_2$, 10 mM Hepes, 20 mM glucose, 24 mM $NaHCO_3$ and 5 mM Na_2HPO_4) at pH 7.4. Cell population obtained by this technique contained ~70% T cells [4]. The platelet-rich plasma was removed with a plastic pipette and transferred into plastic tubes for further utilization. Washed platelets were prepared from platelet-rich plasma by centrifugation for 10 min at 500 g. The platelet pellet was resuspended in HEPES buffer (buffer no. 2, constituted of 145 mM NaCl, 5 mM KCl, 1 mM $MgCl_2$, 10 mM Hepes, 10 mM glucose, pH 7.4) [6]. Cell suspensions with viability level assessed by Trypan blue exclusion, higher than 95%, were only used.

METABOLIC IMPAIRMENT

Metabolic impairment of cells was obtained by serum starvation at temperatures below 37 ^oC. Human platelets and peripheral lymphocytes were kept various time periods (1 – 48 hours) at room temperature (~ 25 ^oC) or at 4 ^oC, without any nutritional supplement (serum, aminoacids or vitamins) in glucose-containing Hepes buffers 2 and 1 respectively. We name “fresh” samples constituted of suspensions of lymphocytes freshly separated within 90 min after blood drawing or of platelets freshly transferred in serum-free buffer from platelet rich plasma within 1 – 4 h after blood drawing.

SAMPLES

Samples were constituted by continuously stirred, thermostated human platelet and peripheral lymphocyte suspensions of cell densities of $2 \cdot 10^7$ cells/ml and $2 \cdot 10^6$ cells/ml, prepared in Hepes buffers 2 and 1, respectively.

LABELING OF CELLS WITH FLUORESCENT LIPID PROBES

$4 \cdot 10^{-3}$ M stock solution of DPH and $5 \cdot 10^{-4}$ M stock solution of TMA-DPH prepared in tetrahydrofuran and dimethylformamide, respectively, were kept at –20 ^oC until use within a month. Human platelets and lymphocytes were labeled with TMA-DPH by incubating them in the measuring cuvette with 1.25 μM dye at 37 ^oC for 3 min at a cell density of $2 \cdot 10^7$ cells/ml and $2 \cdot 10^6$ cells/ml, respectively. For DPH labeling stock solution was dispersed in PBS at a dilution 1:2000 in complete darkness, followed by 1 h continuous stirring of a fluorophore dispersion at 37 ^oC, also in darkness. Cells were labeled by mixing of a suspension of $5 \cdot 10^6$

lymphocytes/ml or of $2 \cdot 10^7$ platelets/ml respectively, with an equal volume of fluorophore dispersion (2 μM DPH in PBS), and incubating for 30 min at 37 °C in darkness. After washing by centrifugation/resuspension in Hepes or HPMI buffer at a concentration of $2 \cdot 10^7$ cells/ml (platelets) and $2 \cdot 10^6$ cells/ml (lymphocytes), respectively, labeled cell suspensions were used immediately.

FLUORESCENCE ANISOTROPY MEASUREMENTS

Steady state fluorescence and anisotropy measurements were carried out in a Perkin-Elmer MPF 44B spectrofluorimeter or in a Jobin-Yvon SpectroFluo JY3 spectrofluorimeter, equipped with thermostatted cell holders, stirring devices, Polaroid HN polarizers and connected to IBM PC computers using appropriate data acquisition software: SCOPE and EASYEST, respectively. The excitation and emission wavelengths were selected 340 nm / 425 nm and 355 nm / 430 nm for TMA-DPH and DPH, respectively. A BG12 filter placed in front of the exit slit of the sample compartment protected the detector from dispersed laser light. Steady state fluorescence anisotropy values (r) were obtained by quasi-simultaneous (within 12 s) measurements of the intensity components I_{VV} and I_{VH}., where VV and VH stand for vertical/vertical (parallel) and vertical/horizontal (perpendicular) positions of the excitation and emission polarizers, respectively. A correction factor $G = \frac{I_{HV}}{I_{HH}}$ for unequal transmission by the optical elements of the vertically and horizontally polarized intensity components was also determined and thus the **steady-state fluorescence anisotropy** values were calculated every 20 – 25 s according to the formula:

$$r = \frac{I_{VV} - G \cdot I_{VH}}{I_{VV} + 2 \cdot G \cdot I_{VH}} \qquad (1)$$

The small autofluorescence of cells and the unavoidable scattered light contribution, determined by measuring unlabeled controls under the same experimental conditions as samples, were subtracted from each intensity component.

The **lipid order parameters** in the core and in the polar headgroup region of the plasma membrane bilayer, S^{DPH} and $S^{TMA\text{-}DPH}$, were computed as functions of limiting initial r_0 and long-time r_∞ values of the fluorescence anisotropy:

$$S^{DPH} = \sqrt{\frac{r_\infty^{DPH}}{r_0}} \quad \text{and} \quad S^{TMA-DPH} = \sqrt{\frac{r_\infty^{TMA-DPH}}{r_0}} \qquad (2)$$

where $r_0 = r_0^{DPH} = r_0^{TMA\text{-}DPH} = 0.362$, while the limiting long-time fluorescence anisotropy values r_∞ for DPH and for DPH analogs were approximated using the empirical curve obtained by van Blitterswijk *et al*. [25] as

$$r_\infty = 1.270 \cdot r - 0.076 \quad \text{for} \quad 0.13 < r < 0.28 \tag{3}$$

$$r_\infty = 1.100 \cdot r - 0.032 \quad \text{for} \quad 0.28 < r < 0.34 \tag{4}$$

where r represents the DPH and TMA-DPH fluorescence anisotropies respectively, calculated from measured fluorescence intensities according to the formula (1).

Membrane fluidities, f^{DPH} and $f^{TMA\text{-}DPH}$, were expressed as reciprocals of the lipid order parameters.

LASER SOURCE

The radiation source was an AlGaInP/GaAs based semiconductor laser used in the medical practice, Philips CQL806D, with continuous wave output, having emission wavelength of 680 nm, nominal power of 30 mW, elliptical beam size 2.5 mm × 7 mm with speckle area of 17.5 mm^2, divergence 3.5^o and polarization ratio 100:1.

SAMPLE IRRADIATION

Irradiation of the samples was performed using a dedicated experimental set-up and/or directly in a fluorimeter, both equipped with thermostatting and stirring facilities. In the fluorimeter a BG12 filter protected the detector from any scattered laser light. Due to beam divergence of the used laser source, the incident power density values were source-sample distance dependent. At a 2 cm distance from the source the measured incident power was 0.026 W. This resulted in an estimated average incident power density on the 1 cm^2 upper surface of the continuously stirred cell suspension of ~260 W/m^2, which lies in the upper limit region of intensities typically used in low power long wavelength laser therapy. Moving the source 6 cm away from the sample, beam divergence caused an increase in speckle size and in consequence a ~10% loss in the magnitude of power incident on the sample. In these conditions the estimated average incident power density on the 1 cm^2 upper surface of the continuously stirred cell suspension became ~234 W/m^2.

The minimum irradiation time of the continuously stirred cell suspension was 12 s, equal to the time needed to measure all four fluorescence intensities in order to calculate one fluorescence anisotropy value, according to formula (1). With the laser source placed at the 6 cm distance from the sample, the estimated average incident energy density per experimental point, gathered in the presence of laser radiation, was ~2.8 kJ/m^2.

Duration of irradiation – realized previous to or during steady state fluorescence anisotropy measurements – varied between 12 – 600 s, resulting, at a given power density, in energy densities in the range of 2.8 – 140 kJ/m^2.

STATISTICAL ANALYSIS

Anisotropy, lipid order parameter and membrane fluidity values and changes occurred in these parameters under the influence of laser irradiation are presented as *mean*±*S.D.* calculated from at least 3 independent measurements. Unpaired analysis of data series obtained by measurements made on cells various time periods after their transfer in serum-free buffer, before, during and after laser irradiation, was performed by Student's t-test. Significance was accepted at $p < 0.05$.

RESULTS

At 37 ^{o}C the fluorescence polarization of the hydrophobic lipid probe, DPH, was relatively weak in both human platelets and peripheral lymphocytes. The reduced fluorescence anisotropy values of 0.207 ± 0.012 and 0.191 ± 0.022 respectively, indicated relatively reduced order (order parameters: 0.734 ± 0.024 and 0.700 ± 0.047) and corresponding relatively high fluidity (1.363 ± 0.043 and 1.437 ± 0.100) in the core of plasma membrane lipid bilayer in these cells. In same conditions the positively charged lipid probe, TMA-DPH, reported in the headgroup region of the plasma membrane lipid bilayer of human platelets and peripheral lymphocytes average fluorescence anisotropy values of 0.289 ± 0.005, and 0.270 ± 0.009. The corresponding values of the second rank order parameter and fluidity of membrane lipids of 0.896 ± 0.010 and 1.116 ± 0.012, and of 0.855 ± 0.016 and 1.170 ± 0.022, in platelets and lymphocytes respectively, indicate higher order in the headgroup region as compared to the core of the plasma membrane in these cells.

Under the influence of the 680 nm laser irradiation apparently significant changes occur in most of these parameters (Figs. 1 – 5). Metabolically impaired cells with intact plasma membrane (more than 88% Trypan blue excluding, data not shown) appear to be more sensitive to laser irradiation (Figs. 6 – 9), as compared to metabolically intact (less than 20% altered membrane potential, higher than 92% viability, data not shown) controls.

Changes induced are less substantial in the core of the plasma membrane in both cells (Figs. 1–2). The statistical significance of the differences observed is also lower.

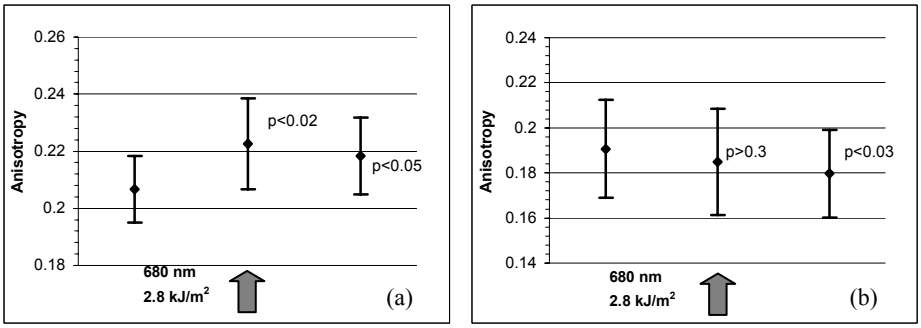

Fig. 1. – DPH fluorescence anisotropy (*r*) data, demonstrating apparently significant laser irradiation effects in human platelets (a) and peripheral lymphocytes (b) exposed to various periods (0–4h) of previous serum starvation.

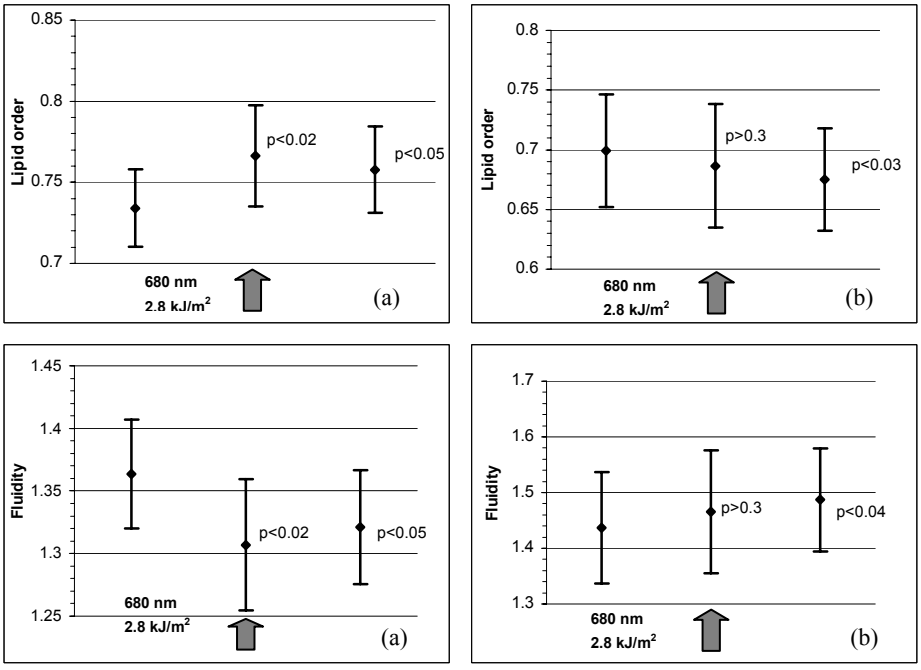

Fig. 2. – Data concerning membrane lipid order (*S*) and fluidity (*f*) in the core of plasma membrane lipid bilayer, demonstrating apparently significant laser irradiation effects in human platelets (a) and peripheral lymphocytes (b) exposed to various periods (0–4h) of previous serum starvation.

Careful experiment design, using cell populations more homogeneous as concerns the treatment parameters, can even cause the loss of statistical significance of irradiation effects (Fig. 3). However – as it can be seen on Fig. 3B –

16. MATKO, J., J. SZÖLLÖSI, L. TRÓN, S. DAMJANOVICH, Luminescence spectroscopic approaches in studying cell surface dynamics, *Quarterly Rev. Biophys.*, 1988, **21**, 479–544.
17. MATKO, J., P. NAGY, Fluorescent lipid probes 12-AS and TMA-DPH report selective, purinergically induced fluidity changes in plasma membranes of lymphoid cells, *J. Photochem.Photobiol. B*., 1997, **40**, 120–125.
18. MOORE, K., G. CALDERHEAD, The clinical application of low incident power density 830 nm GaAlAs diode laser radiation in the therapy of chronic intractable pain: A historical and optoelectronic rationale and clinical review, *J. Optoelectronics,* 1991, **6**, 503–520.
19. OKUMURA, M., T. OKUDA, T. NAKAMURA, YAJIMA M., Acceleration of wound healing in diabetic mice by basic fibroblast growth factor, *Biol. Pharm. Bull.*, 1996, **19**, 530–535.
20. POGREL, M.A., J.W. CHEN, K. ZHANG, Effects of low-energy gallium-aluminum-arsenide laser irradiation on cultured fibroblasts and keratinocytes, *Lasers Surg. Med.*, 1997, **20**, 426-432.
21. SHEFER, G., I. BARASH, U. ORON, O. HALEVY, Low-energy laser irradiation enhances de novo protein synthesis via its effects on translation-regulatory proteins in skeletal muscle myoblasts, *Biochim. Biophys. Acta,* 2003, **1593**, 131–139.
22. SHEFER, G., T.A. PARTRIDGE, L. HESLOP, J.G. GROSS, U. ORON, O. HALEVY, Low-energy laser irradiation promotes the survival and cell cycle entry of skeletal muscle satellite cells, *J. Cell Science*, 2002, **115**, 1461–1469.
23. SZÖLLÖSI, J., Fluidity/viscosity of biological membranes, in: *Mobility and Proximity in Biological Membranes*, Damjanovich, S., J. Szöllösi, L. Trón, M. Edidin, eds., CRC Press, Boca Raton, 1994, pp. 137–208.
24. TUNER, J., L. HODE, *Laser Therapy*, Prima Books, Grängesberg, 2002.
25. VAN BLITTERSWIJK, W.J., R.P. VAN HOEVEN, B.W. VAN DER MEER, Lipid structural order parameters (reciprocal of fluidity) in biomembranes derived from steady-state fluorescence polarization measurements, *Biochim. Biophys. Acta*, 1981, **644**, 323–332.
26. WHEELAND, R.G., History of lasers in dermatology, *Clin. Dermatol.,* 1995, **13**, 3–10.
27. WHEELAND, R.G., Lasers for the stimulation or inhibition of wound healing, *J. Dermatol. Surg. Oncol.,* 1993, **8**, 747–52.
28. YU, W., J.O. NAIM, R.J. LANZAFAME, The effect of laser irradiation on the release of bFGF from 3T3 fibroblasts, *Photochem. Photobiol.* 1994, **59**, 167–70.
29. YU, H.S., K.L. CHANG, C.L. YU, J.W CHEN, G.S. CHEN, Low-energy helium-neon laser irradiation stimulates interleukin-1 alpha and interleukin-8 release from cultured human keratinocytes, *J. Invest. Dermatol.,* 1996, **107**, 593–6.
30. YU, W., J.O. NAIM, R.J. LANZAFAME, Effects of photostimulation on wound healing in diabetic mice, *Lasers Surg. Med.,* 1997, **20**, 56–63.

DRUG INDUCED MEMBRANE EFFECTS IN METABOLICALLY IMPAIRED AND NONIMPAIRED HUMAN T (JURKAT) LYMPHOBLASTOID CELLS

EVA KATONA, GYÖNGYVÉR KATONA**, A. CĂPLĂNUŞI**, MAGDA TUFEANU*, CEZARINA NEGREANU*, DIANA IONESCU**

*Department of Biophysics, "Carol Davila" University of Medicine and Pharmaceutics, Bucharest, Romania
**Department of Medical Biochemistry, "Carol Davila" University of Medicine and Pharmaceutics, Bucharest, Romania

Abstract. Steady-state fluorescence polarization measurements showed that N,N-dimethylaminoethyl hydrochloride esters of phthaloyl-glycine (Pht-Gly) and phthaloyl-leucine (Pht-Leu) induce increase in the lipid order parameter and membrane rigidization, while quaternary ammonium salts of Pht-Gly and Pht-Leu cause diminution of lipid packing density in the polar head-group region and produce fluidization of the human leukemic T cells plasma membrane inner surface. Progressive metabolic impairment of cells leads to changes in plasma membrane properties, modulation, and finally loss of membrane effects of these antibacterial agents.

Key words: N-phthaloyl-aminoacid derivatives, serum starvation, plasma membrane fluidity, lipid order parameter, steady-state fluorescence anisotropy, TMA-DPH.

INTRODUCTION

Plasma membranes of cells are constituted from lipid and protein molecules exhibiting a certain degree of static order and a variety of motional dynamics. Both order and dynamics of membrane components are measurable by spectroscopic techniques [1–4, 6]. Using appropriate lipophilic probes and monitoring changes in their steady state fluorescence anisotropy changes occurring in lipid dynamics and order in various regions of the membrane bilayer, can easily be detected. The technique allows to follow up membrane effects of biologically active chemicals, as well as the influence of cells metabolic state leading to modulation of these effects.

Newly synthesized N,N-dimethylaminoethyl esters of some phthaloyl-aminoacids and their quaternary ammonium salts were described as potent antimicrobial agents having negligible effects on cholesterol containing artificial lipid membranes permeability [5].

Received September, 2004;
in final form April 2005.

ROMANIAN J. BIOPHYS., Vol. 14, Nos. 1–4, P. 29–36, BUCHAREST, 2004

where r_0 = 0.362, while the limiting long-time fluorescence anisotropy values r_∞ were approximated using the empirical curve obtained by van Blitterswijk *et al*. [6] as:

$$r_\infty = 1.270 \cdot r - 0.076 \quad \text{for} \quad 0.13 < r < 0.28 \tag{3}$$

$$r_\infty = 1.100 \cdot \mathrm{r} - 0.032 \quad \text{for} \quad 0.28 < r < 0.34 \tag{4}$$

where r represents the TMA-DPH fluorescence anisotropies, calculated from measured fluorescence intensities according to the formula (1).

Membrane fluidity, f, was expressed as a reciprocal of the lipid order parameter.

The energetic parameter, characteristic of the degree of order in the lipid head-group region of plasma membrane bilayer, was calculated according to a formula analogous with that given by Shinitzky [3]:

$$E_\mathrm{a} = \frac{R \cdot T_1 \cdot T_2}{T_2 - T_1} \cdot \ln \frac{S_{T_1}}{S_{T_2}} \tag{5}$$

TREATMENT OF SAMPLES WITH BIOLOGICALLY ACTIVE COMPOUNDS

Exposure of cells to the action of the studied chemicals was realized by mixing dense cell suspensions with comparable volumes of the compounds concentrated solutions. Final concentration of the active substances in cell suspensions of $1–2 \cdot 10^6$ cells/ml was 1%.

STATISTICAL ANALYSIS

Anisotropy, lipid order parameter and membrane fluidity values and changes occurred in these parameters under the influence of laser irradiation are presented as mean ± S.D. calculated from at least three independent measurements. Unpaired analysis of data series obtained by measurements made on drug treated and control cells, was performed by Student's *t*-test. Significance was accepted at $p < 0.05$.

RESULTS AND DISCUSSION

At 37 °C the positively charged lipid probe, TMA-DPH, reported in the head-group region of the plasma membrane lipid bilayer of Jurkat cells an average fluorescence anisotropy of 0.25 ± 0.01. The corresponding values of the second rank order parameter and fluidity of membrane lipids were 0.81±0.02 and 1.24±0.03

respectively. The values of the same parameters at 25°C were 0.28±0.01, 0.87±0.01 and 1.15±0.02, respectively.

Under the influence of the different newly synthetized drugs the steady-state fluorescence anisotropy of TMA-DPH incorporated in human T lymphoblasts (Jurkat) plasma membrane appeared altered in different manner and to a different extent (Fig. 1 and Table 1).

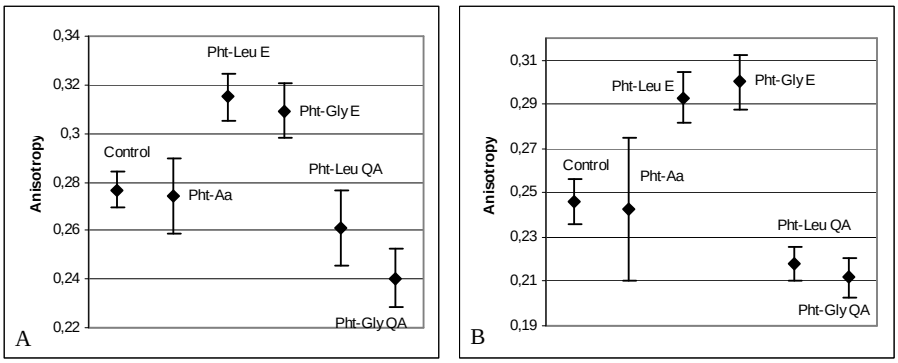

Fig.1. TMA-DPH fluorescence anisotropy (r) data, demonstrating significant drug membrane effects in human T cells, Jurkat, at both room temperature, 25 °C (A) and 37 °C (B).

The inactive source substance – the phtaloyl aminoaminoacid (Pht-Aa) – had no measurable membrane effect at any of these temperatures.

Table 1

TMA-DPH fluorescence anisotropy (*r*) data reporting drug effects at different temperatures on membrane lipid order (*S*) and fluidity (*f*) in the lipid head-group region of plasma membrane of metabolically intact human T cells

		Control	Pht-Aa	Pht-Leu E	Pht-Gly E	Pht-Leu QA	Pht-Gly QA
25 °C	*r*	0.277±0.007	0.274±0.016	0.315±0.010	0.309±0.011	0.261±0.016	0.240±0.012
	S	0.870±0.011	0.864±0.028	0.932±0.016	0.923±0.018	0.840±0.033	0.795±0.026
	f	1.150±0.015	1.158±0.038	1.073±0.018	1.084±0.021	1.193±0.049	1.258±0.040
37 °C	*r*	0.246±0.010	0.243±0.032	0.293±0.012	0.300±0.012	0.218±0.008	0.212±0.009
	S	0.808±0.022	0.798±0.076	0.898±0.018	0.908±0.021	0.745±0.018	0.730±0.022
	f	1.238±0.033	1.262±0.124	1.114±0.023	1.102±0.025	1.342±0.033	1.371±0.042

The statistical significance of induced changes was higher than that corresponding to $p < 0.05$ in cases of all bactericid phtaloyl-aminoacid derivatives at both temperatures. At 37 °C the statistical significance of the observed differences was higher than that corresponding to $p < 0.0005$ in case of all studied